Studies of the high rate coincidence timing response of the STiC and TOFPET ASICs for the SAFIR PET scanner

Jinst

Published by IOP Publishing for Sissa Medialab

Received: *October 3, 2016*
Accepted: *November 13, 2016*
Published: *December 1, 2016*

Studies of the high rate coincidence timing response of the STiC and TOFPET ASICs for the SAFIR PET scanner

R. Becker,[a] **C. Casella,**[a,b] **S. Corrodi,**[a,1] **G. Dissertori,**[a] **J. Fischer,**[a] **A. Howard,**[a] **M. Ito**[a] **and W. Lustermann**[a]

[a] *ETH Zürich — Institute for Particle Physics*
Zürich, Switzerland
[b] *now at University di Milano Bicocca, Italy*

E-mail: simon.corrodi@cern.ch

Abstract: The proposed SAFIR PET detector will measure positron electron annihilations at injected activities up to 500 MBq in a mouse or rat. The system is required to have the best possible timing resolution in order to remove accidental coincidences (randoms) and maximise the image quality for short time frames allowing the possibility of 4-D kinetic modelling of simultaneous PET and MRI for the first time. Two different ASICs, TOFPET and STiC, have been investigated with LYSO crystal scintillators coupled to SiPM detectors and using ^{18}F sources up to 480 MBq. Timing responses are very encouraging with a coincidence time resolution of ∼100 ps measured at low activities, degrading to 130 ps at the foreseen scanner maximum event rate. Sensitivities for single event rates and coincidences are measured and compared with Geant4 Monte Carlo simulations.

Keywords: Electronic detector readout concepts (solid-state); Photon detectors for UV, visible and IR photons (solid-state); Scintillators, scintillation and light emission processes (solid, gas and liquid scintillators); Gamma camera, SPECT, PET PET/CT, coronary CT angiography (CTA)

[1]Corresponding author.

doi:10.1088/1748-0221/11/12/P12001

2016 JINST 11 P12001

Contents

2016 JINST 11 P12001

1 Introduction

The SAFIR (Small Animal Fast Insert for mRi) is being developed to allow simultaneous Positron Emission Tomography (PET) and functional Magnetic Resonance Imaging (fMRI) with excellent temporal resolution. PET images with short time intervals will open up a new paradigm in quantitative 4-D tracer kinetic modelling. However, to achieve fast acquisition times will require the injection of high radio-tracer activities up to 500 MBq into the small animal (mice or rats) together with excellent scanner sensitivity and small images pixel size. To limit random coincidence contributions to the prompt count rate an excellent resolving time of the order of 130 ps[1] is needed [1, 2]. The highly granular detector (2.1 mm crystal width with one-to-one coupling of the crystals to the photo-sensors) results in an expected gamma interaction rate of ~100 kHz/channel. These data have to be handled on a sufficiently fast bus, processed and stored at a photopeak rate of ~40 kHz/channel.

A number of multi-mode Application Specific Integrated Circuits (ASICs) have been developed recently to take advantage of the fast time response of silicon photo-multipliers (SiPMs) [3–7]. Two of these ASICs, STiC [4] and TOFPET [3], have been developed within the EndoTOFPET-US [8]

[1] Sigma of the Gaussian timing distribution.

project and are suitable candidates for the SAFIR scanner due to their state-of-the-art timing resolutions.

In the following, the findings of a high-rate test using ^{18}F-FDG in two equivalent setups with the STiC and the TOFPET ASIC are presented. Particular focus is put on their suitability with respect to time resolution and high-rate capability to determine the applicability of these two ASICs for the SAFIR system.

2 ASIC description

The STiC and the TOFPET chips were decided to be tested with high radioactivities in order to determine their timing performance and data acquisition rate with respect to expectation. Details of the two tested ASICs are described below, a comparison can be found in table 1. Both mixed-mode chips comprise 64 channels with low impedance and provide precise time information together with time-over-threshold (ToT-like) energy measurement. They utilize two adjustable thresholds T and E to maximise timing performance and exclude low energy (Compton) events from the data. The hit time is defined by the rising edge at T-threshold, whereby only signals passing the E-threshold are validated. The energy, provided in a ToT-measurement, is given by the time difference of the falling edge at the E-threshold and the hit time.

2.1 STiC 3.1

The STiC differential input-stage, which could be operated in single-ended mode, provides an adjustment of the photo-sensor bias for individual channels in a range of approximately 700 mV (SiPM DAC). The digital back-end contains two independent Phase Lock Loops (PLL) with a 16-stage voltage controlled ring oscillator (VCO) designed for 625 MHz. Latching the state of this ring oscillator in combination with a coarse counter provides the digitisation of the T- and E-timestamps in variable bins with a mean width of 50.2 ps [9]. The same Time to Digital Converter (TDC) is used for both timestamps. The signal charge is stored on the detector and discharged with a constant current. As a consequence the length of the signal is to first approximation proportional to the charge. This results in a linearised energy measurement despite employing a ToT technique. The T-threshold can be adjusted around the single photon level, whereas the E-threshold covers a much larger range up to SiPM saturation. The chip provides one 160 Mbit/s 8B/10B encoded LVDS link with a hit size of 48-bits and can handle a maximum hit rate of 2.6 Mhits/s/chip. More details can be found in [4, 10].

2.2 TOFPET v1

The TOFPET front-end splits the pre-amplified signal into a time and an energy branch for each channel. The two thresholds, T and E, are adjustable in a range from sub-photon up to approximately 20 photons[2]. The small adjustment range of the E-threshold is an undesired feature and should be corrected in the next generation of the ASIC [11]. A global counter with a nominal frequency of 160 MHz is used to provide a coarse timing measurement. The time between this clock and the

[2]Making use of the possibility to run with $\frac{1}{2}$ or $\frac{1}{4}$ of the gain, the maximum threshold could be increased by a factor 2 or 4. However, this feature was never investigated.

2016 JINST 11 P12001

Table 1. Feature comparison of the two tested ASICs STiC 3.1 and TOFPET v1.

	STiC 3.1	**TOFPET v1**
channels per ASIC	64	64
input mode	differential or single	single
time digitisation	latching of ring oscillator	TAC-ADC chain
"TDC"s per channel	1	8 TACs + 2 ADCs
energy (ToT) linearity	first order linear	non-linear
T-threshold range	~100 fC (sub-photon) up to ~5 pC (~20p)	sub-photon up to ~20p
E-threshold range	above SiPM saturation	sub-photon up to ~20p
LVDS data links	1×160 Mbit/s	2×320 Mbit/s
theoretical hit rate	2.5 Mhits/s/chip	7.5 Mhits/s/chip

rising edge of the signal is measured with a chained TAC-ADC providing a fine time measurement in ~49 ps bins. Arbitration is applied between four time-to-analogue converters (TACs) for de-randomization and digitisation is made by a Wilkinson analogue-to digital converter (ADC) [11]. The data acquisition (DAQ) consists of two LVDS links operating at 160 MHz with double data rate, which results in a maximum raw bandwidth of 640 Mbit/s. Up to 48 hits are streamed 8B/10B encoded in 6.4 µs long frames. The maximum theoretical output rate is thus 7.5 Mhits/s. The operation of the TOFPET is described in depth in [12] and [13].

3 Experimental measurements

3.1 Data acquisition systems

The two ASIC test setups make use of two completely different evaluation-DAQs, which are described in more details below. Both DAQ systems are connected to their corresponding mother boards which provide the bias voltages for the ASICs and SiPMs, reference clocks of 160 MHz and 622.5 MHz (only STiC), 10 MHz Serial Peripheral Interface (SPI) for configuration and the LVDS data links. They can each host two mezzanine boards with two ASICs each. The two mother boards and DAQ hardware were produced by the corresponding developing institutes of the ASICs.[3]

STiC: The STiC DAQ uses a custom FPGA board [14] hosting a Xilinx Spartan 6 to receive the LVDS data stream as well as for the SPI chip configuration. A Cypress EZ-USB FX2LP USB Microcontroller [15] is used for the communication between the FPGA board and the computer. Bulk USB transfer with a block size of 1024 byte results in a data rate of ~650 khits/s (cf. theoretical maximum 850 khits/s[4]). Note that this DAQ event rate is below the 2.5 Mhits/s data rate of the ASIC from the 160 Mbit/s LVDS data links. Due to buffering on the FPGA, the USB saturation can be overcome if less than 8192 events are produced before a full readout of the buffer [16].

[3] STiC: Kirchoff-Institute for Physics, Im Neuenheimerfeld 227, D-69120 Heidelberg; TOFPET: PETsys Electronics, Taguspark, Edificio Technologia I, 26, PT-2740-122 Oeiras.

[4] 1024 Byte/micro − frame / 125 µs/micro − frame / 8 Byte/event · 0.84 (loss due to cypress firmware re-transmission).

2016 JINST 11 P12001

TOFPET: A "PETsys TOF ASIC evaluation kit" was acquired from PETsys Electronics [11]. For the read-out of the ASICs, a Xilinx ML605 Evaluation Kit featuring a Virtex 6 FPGA was connected to the motherboard. The ML605 provides a gigabit ethernet interface which allows full-rate ASIC readout.

3.2 Experimental setup

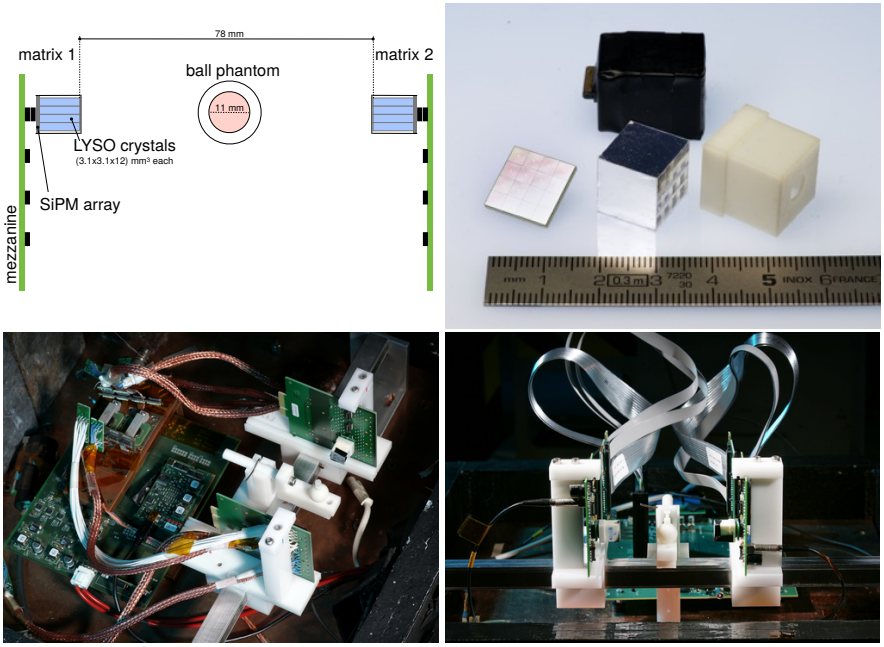

Figure 1. Sketch and pictures of the experimental setup and of the detector components of the two matrices operated in coincidence. Bottom left and right pictures show respectively the STiC and TOFPET test setups.

The coincidence setup comprised two matrices of LYSO crystals coupled to two SiPM arrays facing each other. A spherical phantom (inner diameter = 11 mm; outer diameter = 17 mm) filled with high activity ^{18}F-based tracer ($t_{1/2} \sim 110$ min) was located between the two matrices. Measurements were carried out at the University Hospital Zurich, benefiting from the daily production of FDG by the in-situ cyclotron. Each LYSO crystal matrix was manufactured by Agile Engineering and consisted of a 4×4 assembly of $(3.1 \times 3.1 \times 12)\,\mathrm{mm}^3$ LYSO crystals, with a 100 µm separation (65 µm ESR[5] foil, plus glue). The crystal matrix was one-to-one coupled to a 4×4 SiPM array, Hamamatsu S12642-0404PB-50,[6] together with optical grease (Bicron BC-630). Two identical thermally stable light-tight boxes were used. The two matrices were mounted at a relative face-to-face distance of 7.8 cm with the phantom in the middle as shown in figure 1. The matrices for the TOFPET test were directly coupled to the mezzanine board, whereas for the STiC setup passive connection boards were utilised together with 30 cm long twisted pair cables. The same matrices (crystals and SiPMs) were used alternatively in each of the two configurations in equivalent geometrical arrangements.

[5]Vikuiti 3M Enhanced Specular Reflector.

[6]MPPC array of 4×4 channels, discrete channel type with TSV, $3 \times 3\,\mathrm{mm}^2$ per channel, 50 μm cells size, chip on board package with connector.

2016 JINST 11 P12001

The 64-channel ASICs were only partially loaded by the two matrices. For the TOFPET test, 32 channels were readout with one matrix per chip. The STiC test used a single chip for both matrices, but with two independent PLLs (one per matrix) and only 22 out of the 32 channels were recorded. The optimum SiPM bias working point and thresholds were chosen from measurements with low activity ^{22}Na sources. Bias resistors were employed in both setups: one per mezzanine board in the TOFPET ($R = 270\,\Omega$) and one per SiPM channel ($R = 10\,\mathrm{k}\Omega$) for the STiC. At high rate the expected current results in a voltage drop across these resistors. An external compensation was applied according to the measured total current in order to maintain a constant SiPM bias voltage and thus gain as a function of source activity. For the STiC channels this required bias tuning (SiPM DAC) to be applied prior to the high rate test to equalise the individual currents for all channels.

High rate tests were performed by injecting the spherical phantom (volume 0.7 cm^3) with up to 480 MBq of FDG and then measuring periodically as the activity decreased.

3.3 Monte Carlo simulation

A full simulation of the experimental set-up was made using the Geant4 toolkit [17–19] release 10.3 BETA. The complete detector geometry including the SiPMs, interfaces and reflective foils was implemented. Phantom misalignment was tuned to reproduce the line of response distribution observed in the STiC setup. The radioactive module was used to generate decays within the phantom, the resulting positron interacted and annihilated in the surrounding material. The tracked gammas can then interact within the LYSO crystals and the resulting scintillation process produces optical photons which are then ray-traced back to the SiPM surface. The photon hits with their time distribution are convoluted with a read-out electronics response function. The output is processed to give a series of timestamps and ToTs (energy) which are equivalent to the real data. An image of 100 simulated events is shown in figure 2. To simulate the high rate environment together with full ray-tracing required a significant computation time that was obtained at the CSCS facility.[7]

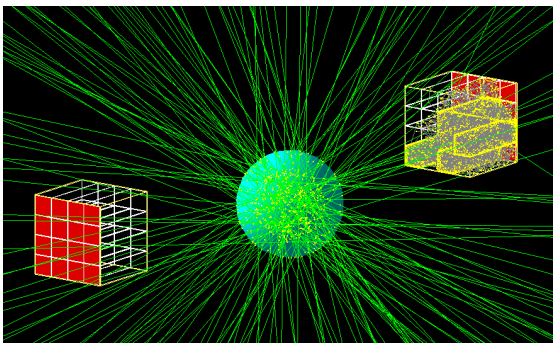

Figure 2. The Geant4 simulated geometry together with the decay of 100 ^{18}F nuclei.

3.4 Data analysis

The same analysis algorithm and cuts are used for the data acquired with the two different ASICs. In a first step a gaussian fit is performed to the photopeak of each channel as shown in figures 6 and 7. Out

[7]CSCS - Swiss National Supercomputing Centre, Via Trevano 131, 6900 Lugano, Switzerland.

2016 JINST 11 P12001

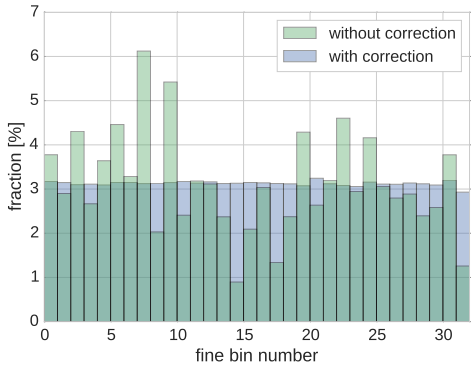

Figure 3. STiC fine bin (latched VCO state) distribution of T-timestamps with and without correction for the different fine bin sizes.

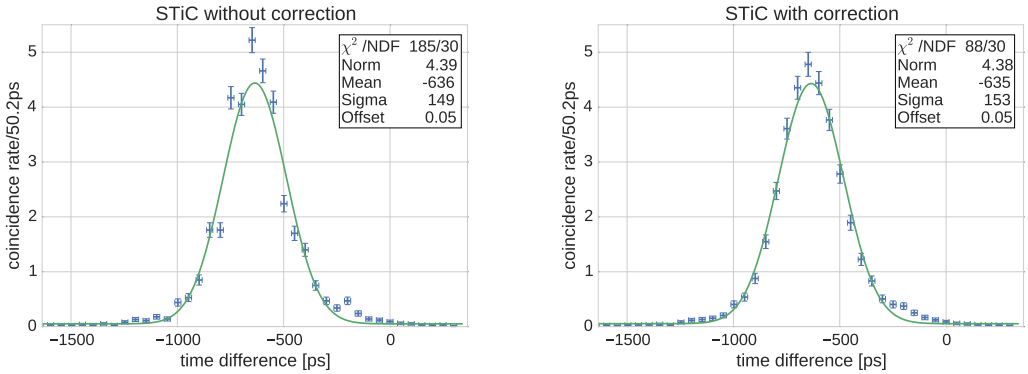

Figure 4. Time difference distribution of one pair of crystals in the STiC setup. In both figures the non-uniform bin sizes are corrected for (figure 3). The left plot is without and the right with smearing according to the associated uncertainties.

of all hits with energies within $\pm 1.5\sigma$ of this photopeak fit all coincidences inside a sliding 10 ns time window are chosen. All combinations are kept. Note that this results in slightly different absolute energy cuts due to the non-linear ToT behaviour of the TOFPET and the different intrinsic energy resolutions of the two ASICs. The time difference of such coincidence events in a given channel pair determine the Coincidence Time Resolution (CTR) of this pair. The non-uniform bin widths in the STiC, as described in chapter 2.1, are taken into account as shown in figure 3. Furthermore, each time difference is smeared out by its uncertainties to randomise quantisation errors due to the finite and different bin sizes. Figure 4 shows a time difference distribution of one pair with (right) and without (left) this smearing. In a last step the CTR is determined by the width (σ) of a gaussian distribution. The following function is fitted in the range of $\pm 6\sigma$ around the CTR peak (μ):

$$P(\Delta t) = \mathrm{A} \cdot e^{\frac{-(\Delta t-\mu)^2}{2\sigma^2}} + \mathrm{c} \tag{3.1}$$

where A is a normalisation and a constant offset, c, is introduced to take into account accidental coincidences. Examples can be found in figure 11.

2016 JINST 11 P12001

4 Results and discussion

Compared to the SAFIR reference design [1, 2], the high rate test setup employed crystals of larger cross section, 3.1 mm × 3.1 mm vs. 2.1 mm × 2.1 mm, and with a smaller face-to-face separation, 7.8 cm vs. 13.8 cm. The 500 MBq target activity of the SAFIR scanner corresponds to ~80 MBq activity in the ball phantom of the high rate test setup in terms of channel occupancy, referred to as *SAFIR-equivalent* conditions.

4.1 DAQ rates

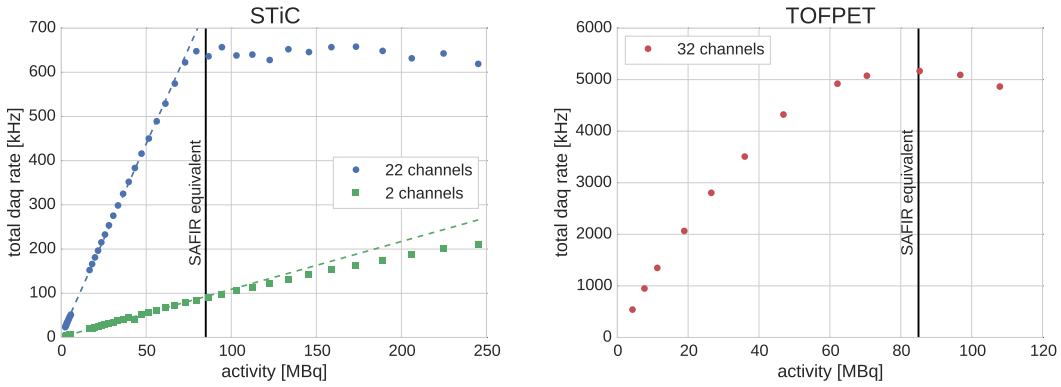

Figure 5. Total DAQ hit rate of the STiC (left) and TOFPET (right) setups plotted as a function of activity within the phantom. The corresponding DAQ rate saturation of ~650 khit/s for STiC (blue) and ~5.2 Mhit/s for TOFPET (red) are clearly identifiable.

Figure 5 shows the total DAQ hit rate at different activities for the two setups. The STiC setup (left plot) DAQ response shows a linear increase of rate with activity up to saturation at ~650 khit/s if 22 channels (blue) are operated on the same ASIC. This corresponds to a limit of ~30 khit/s/channel. This is consistent with the expected maximum rate due to the utilized USB link between the FPGA and the computer. If only two channels (green) are operated saturation is not reached during this test. The non-linear behaviour at high activities is caused by a bias resistor voltage drop resulting in smaller SiPM gain. Consequently, the effective ToT energy threshold is slightly increased at these activities.

The TOFPET setup utilises two ASICs each loaded with 16 channels. Figure 5 (right plot) shows the total DAQ rate with a continuously increasing event loss up to a saturation of ~5.2 Mhit/s. This corresponds to a saturated value of ~2.7 Mhit/s/ASIC or ~160 khit/s/channel. The much higher hit rate in TOFPET with respect to STiC at the same activity is caused by the lower energy threshold in this ASIC.

4.2 Energy spectrum

Figures 6 and 7 show typical ToT spectra from a single channel, as acquired with the STiC and TOFPET setups respectively, at the SAFIR equivalent activity. In both cases the shown crystal is one selected from the four central ones inside the matrix, considering this as the most representative of the SAFIR conditions in terms of the contribution received from Compton scattering events in the neighbours.

2016 JINST 11 P12001

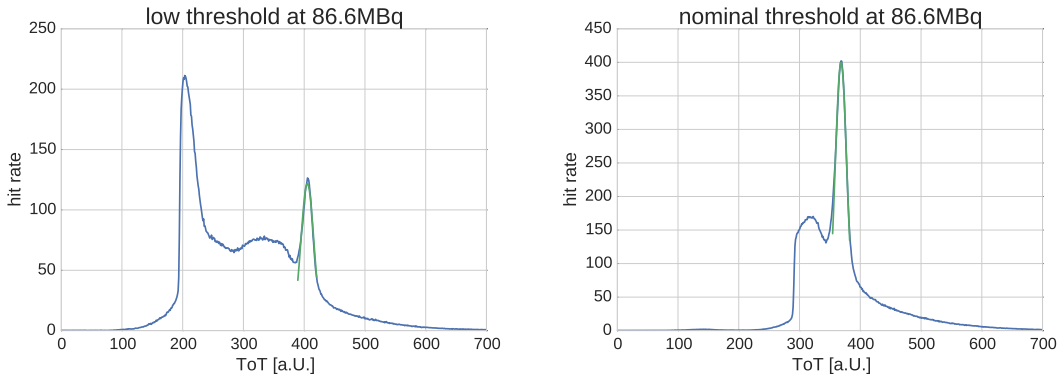

Figure 6. Typical ToT spectra of a single channel, as acquired by the STiC setup, at the SAFIR equivalent activity for both low energy threshold (left) and at the nominal energy threshold (right).

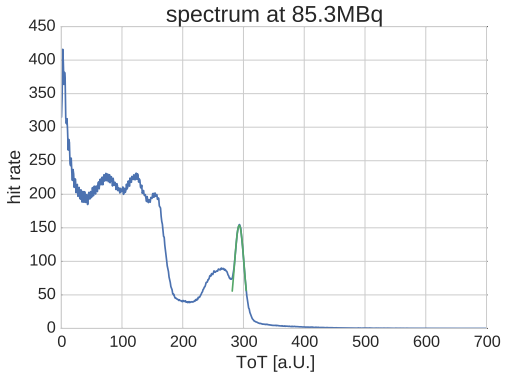

Figure 7. Typical ToT spectra of a single channel, as acquired by the TOFPET setup, at the SAFIR equivalent activity.

In case of STiC (figure 6), ToT spectra at two different energy threshold values are shown. The nominal running conditions (right) correspond to the high energy threshold in which only the photopeak and a small part of the Compton scattering spectrum are retained. A dedicated run at low energy threshold showed a significant contribution in the spectrum from low energy hits, which is also confirmed by the ToT spectra acquired with the TOFPET setup (figure 7), in which the energy validation threshold cannot be put much higher than $\sim$ 20 photons. The low energy artefacts in the ToT spectrum are a result of the maximum settable thresholds on the E threshold. A geometrical correlation among neighbouring channels is observed.

There is a noticeable effect of pileup in the ToT spectra with an excess of events with energies larger than the photopeak, which is more pronounced in the STiC due to the slower pulse-shape.[8]

4.3 Event rate

The observed mean event rate for hits with ToT-values $\pm 1.5\sigma$ around the photopeak fit (top) and values at or larger than the photopeak ($E > E_{\text{photopeak}}$) (bottom) are shown in figure 8 for the STiC (left) and TOFPET (right). A different rate is observed between the two matrices which can be

[8]This can be suppressed by adjusting the STiC running parameters but this configuration was not tested here.

2016 JINST 11 P12001

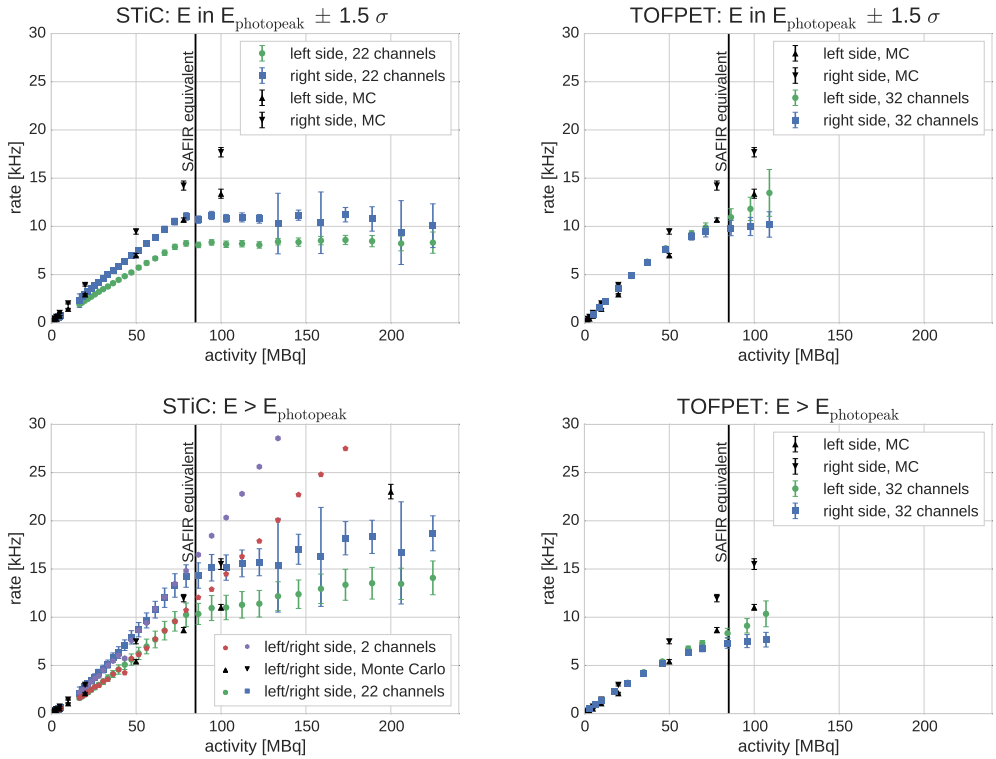

Figure 8. Rate of events with energies $\pm 1.5\sigma$ around the photopeak fit (top) and values at or larger than the photopeak ($E > E_{\text{photopeak}}$) (bottom) for STiC (left) and TOFPET (right). Blue and green points belong to oppositely sided channels. "MC" stands for Monte Carlo simulation.

explained by a small misalignment and offset in the phantom with respect to the detectors. Since there are ToT non-linearity and SiPM saturation effects in both setups the rate of hits with energies larger than the photopeak ($E > E_{\text{photopeak}}$) are used for comparison, which removes a dependency on the gaussian assumption for the shape of the photopeak. This latter measure is E-threshold independent and provides a comparison between the two ASICs and Geant4 simulations. Note that at high activities it is possible for events with energy deposits smaller than the peak position to migrate into the applied cut due to pile-up.

The equivalent expected selected event rate for the SAFIR scanner activity would correspond to ~10 kHz/channel for events inside a $\pm 1.5\sigma$ energy cut. Summation of greater than photopeak events gives an estimate of the true singles rate to be ~225 Hz MBq^{-1}. The single event rates in the two ASICs agree well with expectations and the Geant4 Monte Carlo simulations.

The coincidence event rate was determined for all pairs between the two matrices and is shown graphically in figure 9. The left plot shows data for 18.2 MBq taken with the STiC setup, whilst the right is from the simulation. The occupancy of channel pairs in coincidence is broadly distributed due to the phantom volume being smaller than the matrix resulting in rates below 1.2 Hz MBq^{-1} for golden[9] photopeak events. An overall scaling of the STiC's coincidence rate with respect to Monte Carlo in under further investigation.

[9]Here golden refers to events which have a direct line of response to the source in the context of PET imaging, i.e. photopeak events.

2016 JINST 11 P12001

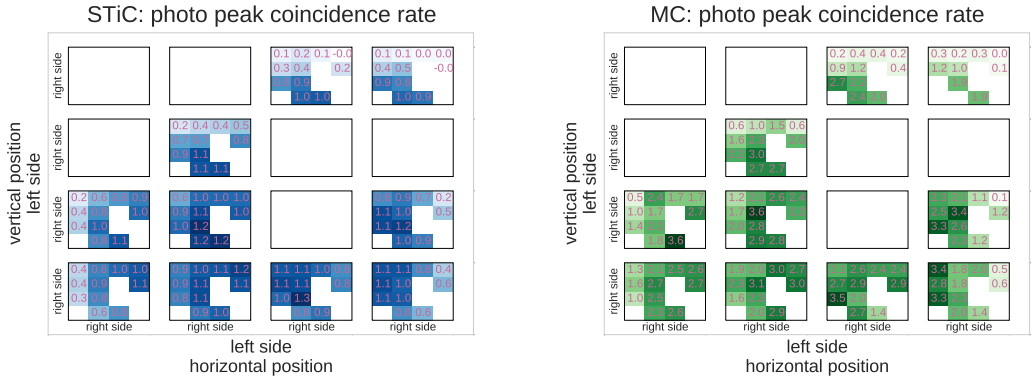

Figure 9. Measured (left) and simulated (right) coincidence event rates per activity for channel pairs between matrices at low activity. The large boxes correspond to one side, whilst the smaller internal boxes correspond to every channel paired with the other. The number in the box is the normalised "golden" event rate in Hz MBq^{-1}. The misalignment of the source with respect to the matrices is clearly visible. The empty (white) boxes correspond to coincidence pairs at least one channel was switched off.

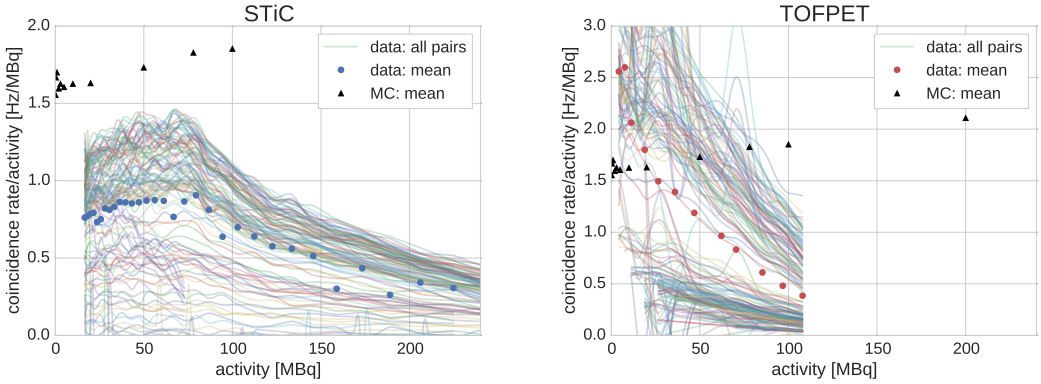

Figure 10. Measured coincidence rate for selected hits greater than photopeak for all channel pairs normalised to photopeak events per second per MBq with Monte Carlo (black) for the STiC setup (left) and the TOFPET setup (right). For better clarity the data (all pairs) is smoothed with a Savitzky-Golay-Filter. In the STiC case the distribution is flat up to ~80 MBq, decreasing for higher activities due to the saturation of the DAQ system. The TOFPET setup shows increasing event loss with activity.

Figure 10 shows the measured coincidence rate for events built with hits having an energy greater than the photopeak for both setups. All channel pairs are normalised to the number of photopeak events per second per MBq. In the STiC case the distribution is flat up to ~80 MBq, and degrades thereafter due to the saturation of the DAQ system. An overall scaling is observed. The TOFPET setup shows too many coincidences for low activities which then show substantial losses as a function of activity. The arithmetic mean of all pairs is plotted in order to facilitate comparison between Monte Carlo and data.

4.4 Timing response

The CTR was determined for both ASICs and is shown in figures 11, 12 and 13 for a sample channel, all channels and as a function of activity respectively. The time difference is not centred

2016 JINST 11 P12001

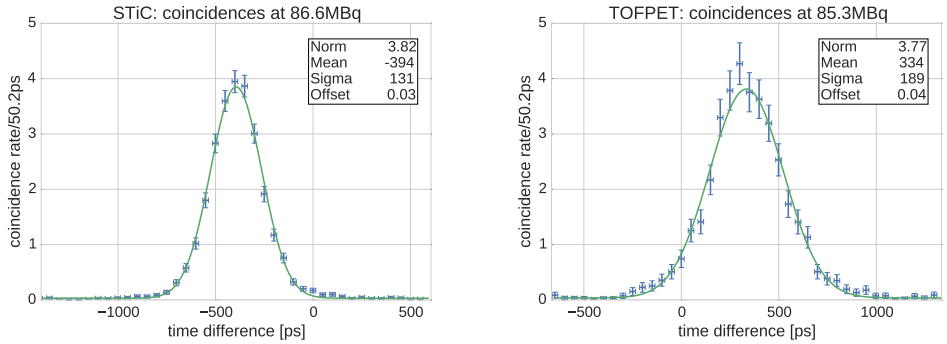

Figure 11. Time differences for two pairs in the middle of the matrix acquired with STiC (left) at 86.6 MBq and TOFPET (right) at 85.3 MBq, i.e. ~SAFIR equivalent. The Coincidence Time Resolution (CTR) is given by the sigma of the fitted function 3.1. Note that the scale of the axes are the same for both plots.

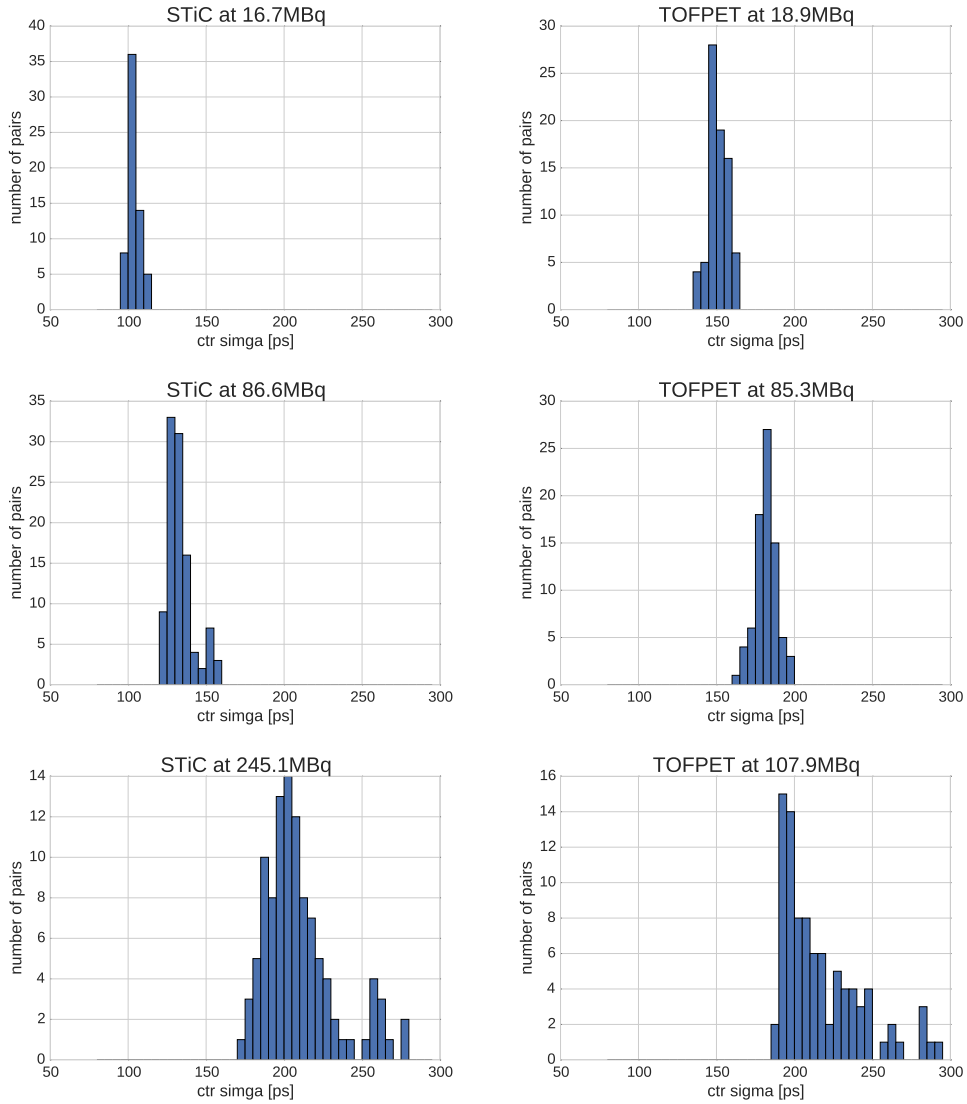

Figure 12. The CTR distribution of all channel pairs for STiC (left) and TOFPET (right) at different activities: ~17 MBq (top), ~85 MBq (middle), 244.1 MBq respectively 107.8 MBq (bottom).

2016 JINST 11 P12001

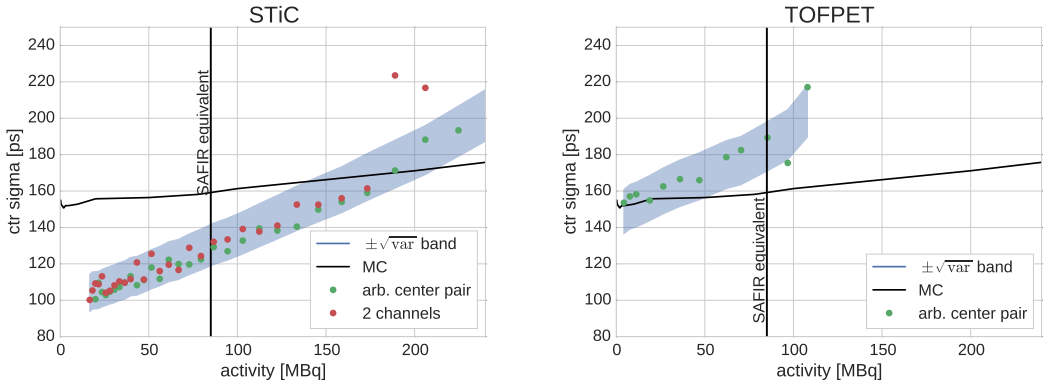

Figure 13. The CTR as a function of activity for STiC (left) and TOFPET (right). The blue band shows the standard deviation ($\sqrt{(\text{var})}$) about the mean of the CTR distributions shown in figures 12. One channel pair in the middle of the matrix is shown in green as well as the results for the 2 channel run in the STiC setup (red).

at zero due to the relative readout time of the two channels. The distribution for all channels is shown for three different activities: ~17 MBq, ~85 MBq (SAFIR equivalent), and ~245 MBq for the STiC and ~108 MBq for the TOFPET measurements. The CTR as a function of activity demonstrates a linear degradation with increasing activity for both setups. Running with different configurations (thresholds, SiPM bias, source distance and number of biased channels) does not improve the situation. This effect can be partially reproduced in simulation if pulse-shape, pile-up effects, dark counts and baseline correction are taken into account. This is still under investigation.

5 Conclusions

It has been demonstrated that both ASICs, STiC and TOFPET, are capable of handling the expected single channel rates (~100 kHz/channel) expected for an activity of 500 MBq in the proposed SAFIR scanner (figure 8). However, the coincidence rates in the TOFPET show a highly non-linear behaviour as a function of activity. It should be noted that the current version does not allow a suffienctly high energy validation threshold to discard undesired hits already on the ASIC. This should be rectified in the next generation of the ASIC. For a function of activity no significant coincidence event loss is observed in the STiC measurements up to the USB-DAQ saturation level. The time resolution of coincidences at ~80 MBq (SAFIR equivalent) is determined to be 130 ps and 189 ps for the STiC and TOFPET respectively. A linear degradation of CTR is observed as a function of increasing activity. This effect is under further investigation but can be partially reproduced in simulations.

A prototype system featuring the STiC is being built to investigate more thoroughly the suitability of the ASIC to the SAFIR insert for an MR scanner.

Acknowledgments

This work was supported by the ETH Zurich Foundation through ETH Research Grant ETH-30 14-2.

2016 JINST 11 P12001

References

[1] R. Becker et al., *Monte-carlo simulation based estimation of necr, sensitivity, and spatial resolution of a novel preclinical pet insert for mr*, *Nuclear Science Symposium and Medical Imaging Conference (NSS/MIC)* (2015) 16357003.

[2] R. Becker et al., *The SAFIR experiment: Concept, status and perspectives*, submitted to *Nucl. Instrum. Meth. A* (2016).

[3] M. Rolo et al., *A 64-channel ASIC for TOFPET applications*, *IEEE Nuclear Science Symposium and Medical Imaging Conference Record (NSS/MIC)* (2012) 1460.

[4] H. Chen et al., *A dedicated readout ASIC for Time-of-Flight Positron Emission Tomography using Silicon Photomultiplier (SiPM)*, *IEEE Nuclear Science Symposium and Medical Imaging Conference (NSS/MIC)* (2014) 15854001.

[5] I. Sacco, P. Fischer and M. Ritzert, *PETA4: a multi-channel TDC/ADC ASIC for SiPM readout*, 2013 *JINST* **8** C12013.

[6] S. Ahmad et al., *Triroc: A multi-channel sipm read-out asic for pet/pet-tof application*, *IEEE Trans. Nucl. Sci.* **62** (2015) 664.

[7] LHCb SciFi Tracker collaboration, D. Gascon, H. Chanal, A. Comerma, S. Gomez, X. Han, J. Mazorra et al., *PACIFIC: A 64-channel ASIC for scintillating fiber tracking in LHCb upgrade*, 2015 *JINST* **10** C04030.

[8] EndoTOPFET-US Proposal, *Novel Multimodal Endoscopic Probes for Simultaneous PET/Ultrasound Imaging for Image-Guided Interventions*, European Union 7th Framework Program (FP7/2007–2013).

[9] M. Ritzert, *Development and Test of a High Performance Multi Channel Readout System on a Chip with Application in PET/MR*, Ph.D. Thesis, Heidelberg University, 2014.

[10] T. Harion, *The STiC ASIC: High Precision Timing with Silicon Photomultipliers*, Ph.D. Thesis, Heidelberg University, 2015.

[11] PETsys Electronics SA, *PETsys TOF ASIC evaluation kit*, 2015, http://www.petsyselectronics.com/web/website/docs/products/product2/FlyerPETsysElectronics-07.2015-v7.pdf.

[12] PETsys Electronics SA, *TOFPET ASIC v1 Short Data Sheet, 1.2*, 2014, http://www.petsyselectronics.com/web/website/docs/products/product1/TOFPETv1_ShortDatasheet_1v2.pdf.

[13] M. Rolo et al., *Tofpet asic for pet applications*, 2013 *JINST* **8** C02050.

[14] T. Pfeil, *Exploring the Potential of Brain-Inspired Computing*, Ph.D. Thesis, Heidelberg University, 2015.

[15] Cypress Semiconductor, *EZ-USB FX2LP USB Microcontroller High-Speed USB Peripheral Controller*, 2015, http://www.cypress.com/file/138911/download.

[16] T. Harion et al., *STiC: a mixed mode silicon photomultiplier readout ASIC for time-of-flight applications*, 2014 *JINST* **9** C02003.

[17] GEANT4 collaboration, S. Agostinelli et al., *GEANT4: A Simulation toolkit*, *Nucl. Instrum. Meth.* **A 506** (2003) 250.

[18] J. Allison et al., *Geant4 developments and applications*, *IEEE Trans. Nucl. Sci.* **53** (2006) 270.

[19] J. Allison et al., *Recent developments in Geant4*, *Nucl. Instrum. Meth.* **A 835** (2016) 186.

2016 JINST 11 P12001